RELATIVISTIC CORRECTIONS IN

HEAVY ION ELASTIC

SCATTERING

A Thesis

By

George Phillip Robinson

RELATIVISTIC CORRECTIONS IN

HEAVY ION ELASTIC

SCATTERING

A Thesis

By

George Phillip Robinson

Approved by:

Adviser: Carlos Bertulani

Committee: Bao-An Li

                                            William Newton

Head of Department: Matt Wood

Dean of the College: Brent Donham

Dean of Graduate Studies: Mary Beth Sampson

ABSTRACT

RELATIVISTIC CORRECTIONS IN

HEAVY ION ELASTIC

SCATTERING

George Phillip Robinson, MS
Texas A&M University-Commerce, 2017

Advisor: Carlos Bertulani, PhD

Relativistic effects of heavy ion scattering were investigated at interme-
diate collision energies, at or above about 50 MeV/n. Two methods for
evaluating these effects were compared for their validity. The first method
involves a full account of the retardation of the Coulomb potential by solu-
tion of the covariant equations of motion for charged particles. The second
method involved the expansion of the effective Lagrangian, including the elec-
tromagnetic Darwin Lagrangian, in orders of (v/c). This study allowed for
the determination of the degree of involvement of effects such as relativistic
magnetic interactions, kinematic corrections, and relativistic mass increase
in the motion of the heavy charge particles. It was shown that the numeric
solutions of the coupled differential equations presented were not necessary as
the analytic formulations sufficiently describe all of the scattering parameters
needed for nuclear experimentation.

ACKNOWLEDGMENTS:

TABLE OF CONTENTS

LIST OF FIGURES

Introduction

In modern radioactive beam facilities, Coulomb excitation is used to probe phenomenon such as dipole polarizeability, pygmy dipole resonance, neutron skin thickness, equations of state of nuclear material, and general nuclear structure. This is done because Coulomb interactions are well understood. Experimentally, it is presumed that Coulomb scattering dominates in small angle scattering especially in the non-head-on elastic scattering of heavy ions. Many of the beam experiments are performed at appreciably high kinetic energies. Due to this, it is crucial that relativistic effects be accounted for in order to properly address relativistic kinematics, any number of possible internal excitations, and any other relativistic reaction dynamics. We sought to investigate the best method to account for relativistic effects in elastic Coulomb scattering of heavy ions. To do this, we explored two different proposed methods for assessing relativistic scattering. The first involved a solution to the covariant equations of motion for a charged particle moving in the electric and magnetic field of another. The second used an expansion of the effective Lagrangian to determine the extent of the relativistic velocities. Both numeric and analytic solutions were given using each method, and both were compared for validity. First however, it is necessary to discuss some background material.

Chapter 1

DARWIN LAGRANGIAN

1.1   Electrodynamics with Retardation

In classical electrodynamics, the Lagrangian for multiple charged particles can be written as follows:

$$L = T - U \tag{1}$$

where T is the kinetic energy, and U is the potential energy.

$$S = \int -mcds = \int Tdt \tag{2}$$

where S is the classical action and $ds = cdt\sqrt{1 - \frac{v^2}{c^2}}$. Therefore:

$$T = -mc^2\sqrt{1 - \frac{v^2}{c^2}} \tag{3}$$

while the potential follows easily from the Force($F = q[\mathbf{E} + (v \times \mathbf{B})]$) as:

$$U = \frac{q}{2}\left(V(r) - \mathbf{A}(r) \cdot \frac{v}{c}\right) \tag{4}$$

(these terms are defined later when we discuss Maxwell's equations, where they are more relevant) bringing us to the final Lagrangian:

$$L = \sum_n \left[-m_n c^2 \sqrt{1 - \frac{v_n^2}{c^2}} + \frac{q_n}{2} \left(\frac{v_n}{c} \cdot \mathbf{A}(r_n) - V(r_n) \right) \right] \tag{5}$$

The Darwin Lagrangian is a term based on the expansion of the classical electrodynamic's Lagrangian above for two relativistic charged particles interacting in free space. It was originally derived in 1920 by Charles Darwin by expansion of the Lienard-Wiechert potential (we differ from the original derivation, as explained below). The term accounts for the reaction of one particle to the magnetic field created by the other. The Darwin Lagrangian follows from the expansion to the order of v^2/c^2, but higher orders are required to account for retardation effects. To find this Lagrangian term, we begin with Maxwells equations:

$$
\begin{aligned}
\nabla \cdot \mathbf{E} &= \frac{\rho}{\epsilon_0} \\
\nabla \cdot \mathbf{B} &= 0 \\
\nabla \times \mathbf{E} &= -\frac{\partial \mathbf{B}}{\partial t} \\
\nabla \times \mathbf{B} &= \mu_0 \mathbf{J} + \mu_0 \epsilon_0 \frac{\partial \mathbf{E}}{\partial t}
\end{aligned}
\tag{6}
$$

We take the curl of the third Maxwell's equation:

$$\nabla \times (\nabla \times \mathbf{E}) = \nabla \times \left(-\frac{\partial \mathbf{B}}{\partial t} \right)$$

$$\nabla(\nabla \cdot \mathbf{E}) - \nabla^2 \mathbf{E} = -\frac{\partial(\nabla \times \mathbf{B})}{\partial t} \qquad (7)$$

$$\frac{\nabla \rho}{\epsilon_0} - \nabla^2 \mathbf{E} = \frac{\partial}{\partial t} \left(\mu_0 \mathbf{J} + \mu_0 \epsilon_0 \frac{\partial \mathbf{E}}{\partial t} \right)$$

making the electric field wave equation with the inclusion of source terms:

$$\Box^2 \mathbf{E} = \frac{\nabla \rho}{\epsilon_0} + \mu_0 \frac{\partial \mathbf{J}}{\partial t} \qquad (8)$$

where $\Box^2 = \nabla^2 - \frac{1}{c^2}\frac{\partial^2}{\partial t^2}$. We can now integrate the Green's function (9) and the sources to find the electric field:

$$G(r,t,r',t') = -\frac{\delta(t-t')}{4\pi\,|r-r'|} \qquad (9)$$

$$\mathbf{E}(r,t) = \int d^3r' dt\, G(r,t,r',t') \left[\frac{\nabla' \rho(r',t')}{\epsilon_0} + \mu_0 \frac{\partial \mathbf{J}(r',t')}{\partial t'} \right] \qquad (10)$$

Through integration by parts, and the unique properties of derivatives of the Greens function$(-\nabla G = \nabla' G)$, we have the following emerge:

$$\mathbf{E}(r,t) = -\nabla V - \frac{\partial \mathbf{A}}{\partial t} \qquad (11)$$

where the scalar potential and the vector potential are respectively defined

by:

$$V(r,t) = \frac{1}{4\pi\epsilon_0} \int \frac{\rho(r', t_r)}{R} d^3r' \tag{12}$$

$$\mathbf{A} = \frac{\mu_0}{4\pi} \int \frac{\mathbf{J}(r', t_r)}{R} d^3r' \tag{13}$$

Similar manipulations of the magnetic field term from Maxwell's equations, and following the same procedure just performed for $\mathbf{E}$ leads to:

$$\mathbf{B}(r,t) = \nabla \times \mathbf{A} \tag{14}$$

In this case, both the $\mathbf{E}$ and $\mathbf{B}$ field equations include the term for the retarded time, $t_r = t - \frac{R}{c}$ where R is the position term, $|r - r'|$ from the Green's function, and c is the speed of light. Additionally, ρ and J are the charge and current distributions respectively.

It is then evident that the E field differs from the electrostatic case by the addition of the time derivative of the vector potential term, while the B field seems to remain the same as the magneto-static case. The B field term does change however, due to the inclusion of the position dependence of the retarded time (as well as R) when the curl is evaluated. This leads to multiple terms through a chain rule, clearly making it different from the magneto-static case.

We will discuss the Lagrangian that arises from this derivation, but this is a convenient place to stop and discuss the Lienard-Wiechert Potential that we use later. So we digress shortly, and will return to this topic after.

1.2 Lienard-Wiechert Potential

Our goal in this section is to find the potential at some location from a charged particle moving through an arbitrary path. So we begin, as we do, with the definition of terms represented in Figure 1.
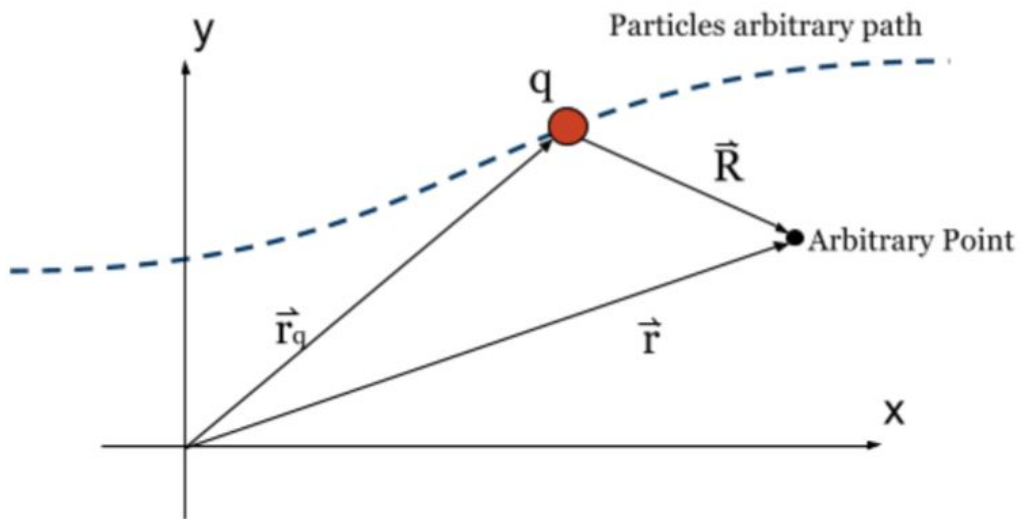
Figure 1: Lienard-Wiechert Potential for a particle moving through an arbitrary path

As shown above, a particle of charge q is moving through an arbitrary path traced by $\mathbf{r}_q$ at a velocity $\mathbf{v}_q(t)$. Additionally, we define, the same as above, a vector from the particle to the point P which we will simplify by calling it $\mathbf{R}$. We can also quite easily define a trivial charge density $\rho(\mathbf{r}, t) = q\delta(\mathbf{r} - \mathbf{r}_q(t))$ and a current $\mathbf{J}(\mathbf{r}, t) = q\mathbf{v}_q\delta(\mathbf{r} - \mathbf{r}_q(t))$. Although we previously derived terms for $V(\mathbf{r}, t)$ and $\mathbf{A}(\mathbf{r}, t)$ only in terms of of a volumetric integral, we will revert back to the time dependent, more generic

versions because we now would like to explicitly solve the time integral rather than take it for granted. We begin with the Scalar Potential:

$$
\begin{aligned}
V(\mathbf{r}, t) &= \frac{1}{4\pi\epsilon_0} \int d^3r' dt' \rho(\mathbf{r}', t') \frac{\delta(t - t' - \frac{R}{c})}{R} \\
&= \frac{q}{4\pi\epsilon_0} \int d^3r' dt' \frac{\delta(\mathbf{r}' - \mathbf{r}_q(t'))\delta(t - t' - \frac{R}{c})}{R} \\
&= \frac{q}{4\pi\epsilon_0} \int dt' \frac{\delta(t - t' - \frac{R_q(t)}{c})}{R_q(t)}
\end{aligned}
\tag{15}
$$

where $\mathbf{R}_q(t) = |\mathbf{r} - \mathbf{r}_q(t)|$, which it should be obvious from this notation that $\mathbf{R}_q$ is time dependent while the original $\mathbf{R}$ was independent of time. So to solve the integral, we must first examine some unique properties of delta functions:

$$
\delta[f(t)] = \sum_i \frac{\delta(t - t_i)}{|f'(t_i)|}
\tag{16}
$$

In this, $f(t)$ is any arbitrary function of t, and at $f(t_i) = 0$ while $f'(t_i) \neq 0$ and in this case, $f(t') = t - t' - \frac{R_q(t')}{c}$. Therefore, $t'_0 = t - \frac{R_q(t_0)}{c}$ and $f(t'_0) = 0$, but t_0 is quite obviously the retarded time t_r. We also need the derivative of f: $f'(t') = \frac{R_q(t') \cdot v_q(t'))}{R_q(t')c} - 1$. Now returning to the integral:

$$
\begin{aligned}
V(\mathbf{r}, t) &= \frac{q}{4\pi\epsilon_0} \int dt' \frac{\delta(t - t_r - \frac{\mathbf{R}_q(t)}{c})}{R_q(t)} \\
&= \frac{q}{4\pi\epsilon_0} \int dt' \frac{\delta(t - t_r)}{(1 - \frac{\mathbf{R}_q(t')}{R_q(t')} \cdot \frac{\mathbf{v}_q(t')}{c})R_q(t)} \\
V(\mathbf{r}, t) &= \frac{q}{4\pi\epsilon_0} \left[\frac{1}{R_q - \frac{\mathbf{R}_q \cdot \mathbf{v}_q}{c}} \right]_{\text{retarded time}}
\end{aligned}
\tag{17}
$$

Similarly, the vector potential $\mathbf{A}$ can be washed through the same steps to obtain the following:

$$\mathbf{A}(\mathbf{r}, t) = \frac{\mu_0 q}{4\pi} \left[\frac{\mathbf{v}_q}{R_q - \frac{\mathbf{R}_q \cdot \mathbf{v}_q}{c}} \right]_{\text{retarded time}} \tag{18}$$

These two equations for the scalar and vector potentials are the Lienard-Wiechert Potentials, but it is no longer necessary to use the q subscript, so we can simplify by writing both as follows:

$$V(\mathbf{r}, t) = \frac{q}{4\pi\epsilon_0} \left[\frac{1}{R(1 - \beta \cdot \hat{R})} \right]_{\text{retarded time}}$$
$$\mathbf{A}(\mathbf{r}, t) = \left[V(\mathbf{r}, t) \frac{\beta}{c} \right]_{\text{retarded time}} \tag{19}$$

1.3 Darwin Lagrangian

Prior to the Lienard-Wiechert Potential explanation, we came up with a term for the $\mathbf{E}$ and $\mathbf{B}$, and from these we can write the Lagrangian for the relativistic interaction of a particle of charge q within an electromagnetic field as:

$$L = -q\nabla V + \frac{q}{c}(\mathbf{v} \cdot \mathbf{A}) \tag{20}$$

where v is the velocity of the charged particle.

Applying the Coulomb Gauge, $(\nabla \cdot \mathbf{A} = 0)$, and removing $\frac{1}{c^2}\frac{\partial^2 \mathbf{A}}{\partial t^2}$

because $\mathbf{A}$ is of order $\frac{v^2}{c^2}$, we can write the following from Maxwells laws:

$$\nabla^2 \mathbf{A} - \frac{1}{c}\left(\nabla \frac{\partial V}{\partial t}\right) = -\frac{4\pi}{c}\mathbf{J}_t \tag{21}$$

where $\mathbf{J}_t$ is the transverse current created by the movement of the second charge. This indicates that the currents divergence is zero throughout. It should be noted that the original derivation done by Darwin did not use this method, however, this method, as performed by Jackson [2], leads to an exact Coulomb potential V and transfers the approximation to the vector potential, $\mathbf{A}$. which becomes:

$$\mathbf{A}(\mathbf{r}) = \int \frac{d^3 r'}{|\mathbf{r}-\mathbf{r}'|}\left(\frac{1}{c}\mathbf{J}(\mathbf{r}') - \frac{1}{4\pi c}\nabla'\frac{V(\partial \mathbf{r}')}{\partial t}\right) \tag{22}$$

We can write $\mathbf{J}(\mathbf{r}')$ for n particles as $q_n \mathbf{v}_n \delta^3(\mathbf{r}'-\mathbf{r}_n)$ and V as $\frac{q_n}{|\mathbf{r}'-\mathbf{r}_n'|}$

$$\mathbf{A}(\mathbf{r}) = \int \frac{d^3 r'}{|\mathbf{r}-\mathbf{r}'|}\left[\frac{q_n \mathbf{v}_n}{c}\delta^3(\mathbf{r}'-\mathbf{r}_n) - \frac{q_n}{4\pi c}\nabla'\left(\frac{\mathbf{v}_n \cdot (\mathbf{r}'-\mathbf{r}_n)}{|\mathbf{r}'-\mathbf{r}_n|^3}\right)\right] \tag{23}$$

Then by integrating by parts, and removing the surface at infinity, while also utilizing the property of greens functions where $\nabla' \approx -\nabla$:

$$\mathbf{A}(\mathbf{r}) = \frac{q_n \mathbf{v}_n}{c\,|\mathbf{r}-\mathbf{r}_n|} + \frac{q_n}{4\pi c}\int d^3 x'\left(\frac{\mathbf{v}_n \cdot (\mathbf{r}'-\mathbf{r}_n)}{|\mathbf{r}'-\mathbf{r}_n|^3}\right)\nabla'\frac{1}{|\mathbf{r}-\mathbf{r}'|} \tag{24}$$

$$\mathbf{A}(\mathbf{r}) = \frac{q_n \mathbf{v}_n}{c\,|\mathbf{r}-\mathbf{r}_n|} - \frac{q_n}{4\pi c}\nabla\int d^3(\mathbf{r}'-\mathbf{r}_n)\frac{\mathbf{v}_n \cdot (\mathbf{r}'-\mathbf{r}_n)}{|\mathbf{r}'-\mathbf{r}_n|^3}\frac{1}{\mathbf{r}'-\mathbf{r}} \tag{25}$$

Finally, by evaluating this non-trivial integral, we reach:

$$\mathbf{A}_n = \frac{q_n}{2cr}v_n + \frac{\mathbf{r}\mathbf{v}_n \cdot \mathbf{r}}{r} \tag{26}$$

where $r = |v\mathbf{r}|$. If we multiply $\frac{q\mathbf{v}}{c}$ to take into account the second (or incidentally, any number by including a subscript to account for the n-th) charged particle, and correct the original free particle Lagrangian by saying that $-mc^2\gamma^{-1} + mc^2 \approx \frac{1}{2}mv^2[1 + \frac{1}{4}\frac{v^2}{c^2}]$ We arrive at the finalized Darwin Lagrangian:

$$\sum_{i \neq j} \frac{1}{2}m_i v_i^2 + \frac{1}{8c^2}m_i v_i^4 + \frac{q_i q_j}{r_{ij}}\left[-\frac{1}{2} + \frac{1}{4c^2}\left(\mathbf{v}_i \cdot \mathbf{v}_j + (\mathbf{v}_i \cdot \hat{r_{ij}})(\mathbf{v}_j \cdot \hat{r_{ij}})\right)\right] \tag{27}$$

where we have used a different index here merely for convenience, and to avoid confusing subscripts.

This Lagrangian is useful when radiation can be neglected, but was originally derived under the assumption of non-relativistic speeds, although that assumption should not be necessary because radiation is due to acceleration. A Lagrangian that both neglects radiation and the assumption of low speeds was proposed by H. Essén [3] and leads to a succinct interaction Lagrangian for the interaction of two particles as:

$$L_{12} = g\left(\frac{v^2}{c^2}\right)\frac{e_1 e_2}{r_{21}}\frac{v^2}{c^2} - \frac{e_1 e_2}{r_{21}} \tag{28}$$

where $g(x) \equiv \frac{1}{1+\sqrt{1-x}}$, $r_{21} = |r_2 - r_1|$, and e is the particle's charge. The

term g can be expended in terms of $\frac{v^2}{c^2}$ and at the limit of $v \to c$, $g(x) = 1$, and the related force is zero. This method allows for all retardation dependencies to be accounted for, which eliminates the assumption of low velocities as required by the original Darwin derivation.

Chapter 2

RUTHERFORD SCATTERING

In May of 1911, Ernst Rutherford published his findings from a scattering experiment in which alpha particles were fired at a thin sheet of gold foil [4]. The atomic models of the time did not conform with the findings of his experiment, as a high percentage of alpha particles were unexpectedly back-scattered at angles greater than 90°. It was this conclusion that led to our current understanding of the ultra-dense positively charged center to atoms, which we now know as the nucleus, surrounded by a large volume, negatively charged space occupied by the electrons. The following are the derivations associated with Rutherford's Scattering model.

Scattering being integral to this subject, it seems prudent to discuss it in some detail. We begin with a few definitions in classical scattering:

An incoming particle, the projectile, is incident on another particle, the target, which we will assume has a very large mass as compared to the incident one so we can neglect recoil of the target. We will discuss removing this assumption later, but for now we will use it to discuss the simpler case. The incoming particle approaches with an impact parameter, b, which we define as the perpendicular distance from the direction of motion of the incoming projectile, and the center of the target. The incident particle will have an initial velocity v_0. After interacting with the target, the projectile

emerges at an angle θ, as measured from the projectile's original direction of motion, and it will have a velocity denoted v_∞ for its velocity as $t \rightarrow \infty$.
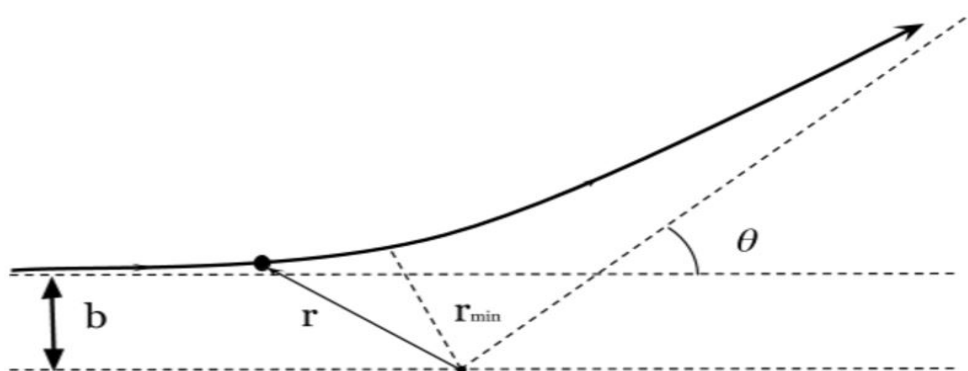
Figure 2: Simple 2-D Scattering

To obtain Rutherford's Scattering equation, we must begin with some assumptions, (in addition to having the mass of the target be much larger than that of the projectile): first, we assume that the only interaction between the projectile and the target is the Coulomb repulsion; this implies azimuthal symmetry. We will also only consider a single projectile and only a single target. And lastly, (and most importantly for this paper) we will consider only non-relativistic speeds (for now).

So from these assumptions and the above definitions, we can now begin to solve for a relationship between the impact parameter b and the scattering angle θ. (these being the best adjustable and measurable parameters respectively for experimentalists in the lab setting). We begin

with the Coulomb Force:

$$F = \frac{Z_1 Z_2 e^2}{4\pi\epsilon_0 r^2} \tag{29}$$

where Ze is the charge of the particle, and $\mathbf{r}$ is the vector that traces the projectile's motion. We then consider the conservation of angular momentum. We know that because angular momentum is conserved, then the angular momentum itself must be equal to some constant, C:

$$|\mathbf{L}| \equiv |\mathbf{r} \times \mathbf{p}| = |mrv|\sin\phi = C \tag{30}$$

Where $\mathbf{L}$ is the angular momentum, $\mathbf{p}$ is the linear momentum, and ϕ is the angle between $\mathbf{r}$ and $\mathbf{v}$. We must then consider the initial angular momentum, where the projectile has not yet experienced any deflection from the Coulomb repulsion. At this time, $\sin\phi = \frac{b}{r}$, so $L_0 = mv_0 b = C$. So we now have a term for the constant C.

Combining the Coulomb Force (29) with our understanding of angular momentum, we can write

$$r^2 = bv_0 (\frac{d\phi}{dt})^{-1} \tag{31}$$

Then by writing the force in Cartesian coordinates.

$$
\begin{aligned}
F_x &= F\cos\phi = \frac{Z_1 Z_2 e^2}{4\pi\epsilon_0 r^2}\cos\phi = \frac{Z_1 Z_2 e^2}{4\pi\epsilon_0 bv_0}\frac{d\phi}{dt}\cos\phi = \frac{mdv_x}{dt} \\
F_y &= F\sin\phi = \frac{Z_1 Z_2 e^2}{4\pi\epsilon_0 r^2}\sin\phi = \frac{Z_1 Z_2 e^2}{4\pi\epsilon_0 bv_0}\frac{d\phi}{dt}\sin\phi = \frac{mdv_y}{dt}
\end{aligned}
\tag{32}
$$

solving this integral for v_i :

$$v_x(\phi) = \frac{Z_1 Z_2 e^2}{4\pi\epsilon_0 mbv_0} \sin\phi + v_0$$

$$v_y(\phi) = \frac{Z_1 Z_2 e^2}{4\pi\epsilon_0 mbv_0}(-\cos\phi + 1) \qquad (33)$$

$$\text{for } 0 \leq \phi \leq \pi - \theta$$

Now we take a look at the conservation of energy, which tells us that the magnitude of the initial and final energy must be equal $(v_0 = v_\infty)$ and at $t \to \infty$, $\phi = \pi - \theta$, so (focusing only on the y-direction):

$$\frac{Z_1 Z_2 e^2}{4\pi\epsilon_0 mbv_0}(-\cos(\pi - \theta) + 1) = v_0 \sin\theta$$

$$\frac{Z_1 Z_2 e^2}{4\pi\epsilon_0 mbv_0}(\cos(\theta) + 1) = v_0 \sin\theta$$

$$\frac{Z_1 Z_2 e^2}{4\pi\epsilon_0 mbv_0} = v_0 \frac{\sin\theta}{\cos\theta + 1} \qquad (34)$$

$$\frac{Z_1 Z_2 e^2}{4\pi\epsilon_0 mbv_0} = v_0 \tan\frac{\theta}{2}$$

one final rearrangement brings us to b as a function of θ.

$$b(\theta) = \frac{Z_1 Z_2 e^2}{4\pi\epsilon_0 v_0^2 m \tan(\frac{\theta}{2})} \qquad (35)$$

Now, we take into account the more appropriate three dimensional version of classical scattering with a beam of incoming projectiles rather than only a single projectile. The projectile incident in a cross-sectional area element $d\sigma = 2\pi b db$ at the cylindrically symmetric impact parameter b

will scatter to a correlating solid angle element $d\Omega = 2\pi \sin\theta d\theta$. From these, we can define a so called differential scattering cross-section, $\frac{d\sigma}{d\Omega}$.
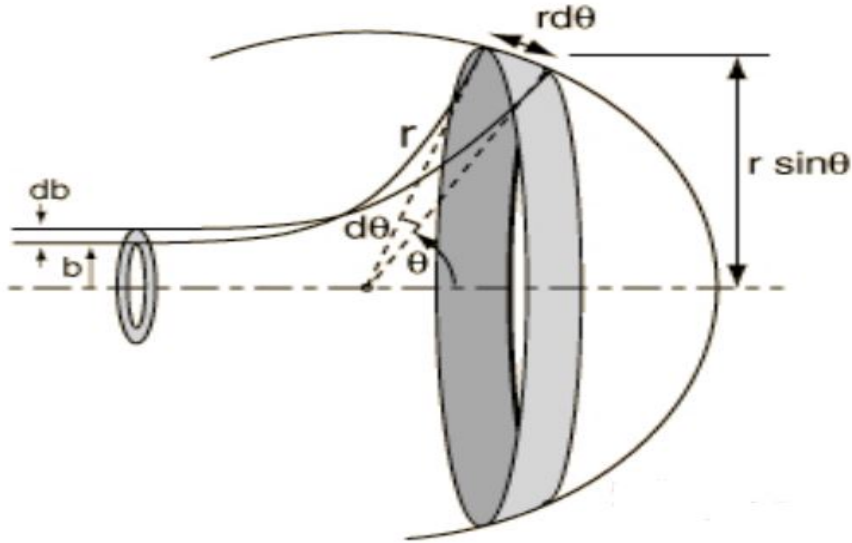
Figure 3: Classical scattering by a central potential

We can say that the number of incoming particles that pass through this differential cross section $d\sigma$ with an intensity, I, must be equal to the number of particles that scatter through the differential solid angle $d\Omega$:

$$I \cdot 2\pi b db = I \cdot \frac{d\sigma}{d\Omega} d\Omega \tag{36}$$

and plugging in what we know about $d\sigma$ and $d\Omega$ we can rearrange to find

an expression for the differential scattering cross section in terms of b and θ:

$$\frac{d\sigma}{d\Omega} = \frac{b}{\sin\theta}\left|\frac{db}{d\theta}\right| \tag{37}$$

Finally, we can plug in $b(\theta)$ (35) and its derivative with respect to θ into (37) to obtain a term for the differential cross section solely in terms of θ.

$$\left|\frac{db}{d\theta}\right| = \frac{Z_1 Z_2 e^2}{16\pi\epsilon_0 K_0 \sin^2(\frac{\theta}{2})} \tag{38}$$

$$\frac{d\sigma}{d\Omega} = \left(\frac{Z_1 Z_2 e^2}{8\pi\epsilon_0 K_0}\right)^2 \frac{1}{2\sin\theta \tan\frac{\theta}{2}\sin\theta} \tag{39}$$

where K_0 is the initial kinetic energy, $K_0 = \frac{1}{2}mv_0^2$. Then by simply using the trigonometric identity: $\sin x = 2\sin\frac{x}{2}\cos\frac{x}{2}$, we arrive at last, at the elegant formula:

$$\frac{d\sigma}{d\Omega} = \left(\frac{Z_1 Z_2 e^2}{16\pi\epsilon_0 K_0}\right)^2 \frac{1}{\sin^4\left(\frac{\theta}{2}\right)} \tag{40}$$

Chapter 3

THE INCLUSION OF RETARDATION IN COULOMB SCATTERING

In 1987, R. Matzdorf and G. Soff published a paper describing the collisions of simi-relativistic heavy ions [5]. In which, they derived a set of coupled equations for the motion for relativistic charged particles. Their method does intentionally neglect radiative corrections. We will use their method in conjunction with a method outlined in a paper written by C. E. Aguiar et al. [6] which is discussed in the following section. Matzdorf begins with the covariant equations of motion that describe a charged particle moving in the external electromagnetic field of another charged particle.

Assuming the projectile is moving in the $\hat{x}$ direction, the covariant equation of motion for the two particle system moving under the influence of their own electric fields and magnetic fields:

$$\frac{dp^\alpha}{d\tau} = \frac{q}{c} F^{\alpha\beta} U_\beta \tag{41}$$

where field strength tensor, $F^{\alpha\beta}$ can be written as:

$$\frac{dp^\alpha}{d\tau} = \frac{q}{c} \begin{pmatrix} 0 & -E_1 & -E_2 & -E_3 \\ E_1 & 0 & -B_3 & B_2 \\ E_2 & B_3 & 0 & -B_1 \\ E_3 & -B_2 & B_1 & 0 \end{pmatrix} U_\beta \tag{42}$$

where p^α is the 4-momentum and U_β is the 4-velocity. τ is the proper time.

The E and B fields are then derived from the Lienard Wiechert potentials (19). Then plugging those back into (42), and produce three relevant equations for the velocities which can be expressed as:

$$\gamma^4 \begin{pmatrix} \gamma^{-2} + u_1^2 & u_1 u_2 & u_1 u_3 \\ u_1 u_2 & \gamma^{-2} + u_2^2 & u_2 u_3 \\ u_1 u_3 & u_2 u_3 & \gamma^{-2} + u_3^2 \end{pmatrix} \dot{\mathbf{u}} = \frac{q^{(p)}\gamma}{m_0^{(p)} c} \begin{pmatrix} E_1^{(t)} - B_3^{(t)} u_2 + B_2^{(t)} u_3 \\ E_2^{(t)} + -B_3^{(t)} u_1 - B_1^{(t)} u_3 \\ E_3^{(t)} - B_2^{(t)} u_1 + B_1^{(t)} u_2 \end{pmatrix}$$

$$(43)$$

This method produces a fourth equation

$\gamma^4(\mathbf{u}, \dot{\mathbf{u}}) = \frac{q^{(p)}}{m_0^{(p)}} - \gamma \left(-E_1^{(t)} u_1 - E_2^{(t)} u_2 - E_3^{(t)} u_3 \right)$, but it provides no additional information, so it is disregarded.

We denote $\mathbf{u} = \frac{\mathbf{v}}{c}$ as the normalized velocity to the speed of light, and $\gamma = (1 - \beta^2)^{\frac{-1}{2}}$. The subscript 1, 2, and 3 denote the direction component as in (x_1, x_2, x_3). In addition, p and t refer to the projectile and target respectively (although the distinction is nonessential because the reference frame can simply be switched to that of the motionless projectile and moving target and all remains the same).

To solve for $\dot{\mathbf{u}}$, a mathematically straightforward matrix manipulation is performed. Although it is straightforward, it is also fairly lengthy, so it is not shown here. By confining the scattering plane to the x-y plane, and solving for $\dot{\mathbf{u}}$ we can reduce the 3×3 matrix to a 2×2 matrix involving only u_1 and u_2 terms.

Using the target's frame of reference, the scalar and vector potentials

can be expressed as:

$$\mathbf{A} = 0$$

$$V = \frac{q}{\mathbf{R}}$$

<div align="right">(44)</div>

Performing a Lorentz transformation into the laboratory reference frame, we find $\mathbf{E}$ and $\mathbf{B}$ can be expressed as:

$$E = q \frac{\mathbf{n}}{\gamma^2 \left[1 - \beta^2 + (\mathbf{n} \cdot \beta)^2\right]^{\frac{3}{2}} R^2}$$

$$B = \beta \times E$$

<div align="right">(45)</div>

Then plugging in the non-vanishing terms, after the restriction to two dimensions, E_1, E_2, and B_3, can be expressed as:

$$E_1 = q \frac{n_1}{\gamma^2 \left[1 - \beta^2 + (\mathbf{n} \cdot \beta)^2\right]^{\frac{3}{2}} R^2}$$

$$E_2 = q \frac{n_2}{\gamma^2 \left[1 - \beta^2 + (\mathbf{n} \cdot \beta)^2\right]^{\frac{3}{2}} R^2}$$

$$B_3 = \beta_1 E_2 - \beta_2 E_1$$

$$\text{where } \beta^2 = \beta_1^2 + \beta_2^2$$

<div align="right">(46)</div>

Lastly, Matzdorf restricts the Coulomb field to be purely classical (i.e. $E = q \frac{\mathbf{n}}{R^2}$ and $B = 0$) and, due to its essentially negligible contribution, on the order of only a single percent difference at speeds less than $0.99c$, the magnetic field's relativistic contribution is omitted.

This leads to the finalized equation for the normalized accelerations

in each direction.

$$\dot{u}_1 = \frac{q^{(p)}q^{(t)}}{m_0^{(p)}\gamma^3} \frac{(\gamma^{-2} + u_2^2)n_1 - u_1 u_2 n_2}{R^2[(\gamma^{-2} + u_1^2)(\gamma^{-2} + u_2^2) - u_1^2 u_2^2]}$$

$$\dot{u}_2 = \frac{q^{(p)}q^{(t)}}{m_0^{(p)}\gamma^3} \frac{(\gamma^{-2} + u_1^2)n_2 - u_1 u_2 n_1}{R^2[(\gamma^{-2} + u_1^2)(\gamma^{-2} + u_2^2) - u_1^2 u_2^2]} \tag{47}$$

where R is the magnitude of the radius vector considering the target at time t, and n represents the unit vector in its respective direction. These equations, (43) and (47), are only soluble numerically as they are obviously interdependent upon one another. The numerical methods are discussed in Chapter 5 and the solutions are discussed in Chapter 6.

In addition to this, the scattering angle can be solved if the target begins at the origin at rest at $t = -\infty$, and the projectile moves originally in the $\hat{x}$ direction, then the solution for the scattering angle can be found by use of the solution to (47) and:

$$\theta(t \to \infty) = \arctan\left(\frac{u_2}{u_1}\right) = \arctan\left(\frac{dy(t)}{dx(t)}\right) \tag{48}$$

The next step, and the ultimate goal of all collision calculations, would be to use these equations to find a relationship between the impact parameter b and the scattering angle θ. This is exactly what we do. Following a method presented by Sommerfeld [7], where they describe the orbital motion of a relativistic electron, and simply change signs to account for the positively charged projectile we wish to use. We then transform the

non-relativistic relationship for the angle, which we denote as ψ, to its relativistic counterpart, ϕ. In this formalism, ψ_0 is simply equal to the arccos of the inverse of the eccentricity. This eccentricity is a function of the non-relativistic angular momentum, and because the goal is to transform everything into the relativistic domain, it was therefore necessary to also rewrite the non-relativistic angular momentum, L_0 in terms of the relativistic angular momentum, $L = L_0\gamma$. This led to the description of ϕ_0 as:

$$\phi_0 = \frac{1}{\sqrt{1 - \frac{(Z_p Z_t e^2)^2}{c^2 L^2}}} \arccos\left(\frac{\frac{Z_p Z_t e^2}{L v_\infty}}{\sqrt{1 + \left(\frac{Z_p Z_t e^2}{L v_\infty}\right)^2}}\right) \tag{49}$$

For succinctness, the simplification, $k(b) = \frac{Z_p Z_t e^2}{L v_\infty} = \frac{d}{2b}\sqrt{1 - \beta^2}$ is made. The parameter d is defined as the collision diameter as: $d = \frac{2 Z_p Z_t e^2}{m_0^{(p)} v_\infty^2}$. This leads to the condensation:

$$\phi_0 = \frac{1}{\sqrt{1 - k(b)^2 \beta^2}} \arccos\left(\frac{k(b)}{\sqrt{1 + k(b)^2}}\right) \tag{50}$$

A conversion from ϕ_0 into θ,

$$\theta = \pi - \frac{2\operatorname{arccot}(k(b))}{\sqrt{1 - k(b)^2 \beta^2}} \tag{51}$$

and plugging this into a rearranged (37) where $\frac{db}{d\theta} = \frac{dk}{d\theta}\frac{db}{dk}$. This produces

the ultimate goal of this endeavor:

$$\frac{d\sigma}{d\Omega} = \frac{b^2}{\sin\theta} \left| \frac{[1+k(b)^2][1-k(b)^2\beta^2]}{2[1+k(b)^2]k(b)^2\beta^2\left(\frac{\pi-\theta}{2}\right) - 2k(b)\sqrt{1-k(b)^2\beta^2}} \right| \tag{52}$$

It is this, equation (52), and the equations of normalized velocity components, equations (47), that are numerically evaluated in [5] and by ourselves. Matzdorf additionally claims an accuracy of 10^{-4} in a collision of a proton with a Uranium atom.

Although it was passed over without comment earlier, the magnetic field contribution, or more appropriately, the lack thereof, should be discussed. Matzdorf showed that the magnetic field does not contribute heavily enough to the motion of the relativistic motion of charged particles to be considered on the range from $0.1c$ to $0.99c$. This in and of itself is not exceptionally interesting, but it has intriguing consequences. The relativistic mass correction must then be quite significant. They reported this specifically for $Xe + U$ collisions.

Chapter 4

SOLUTION OF THE ELECTROMAGNETIC TWO-BODY

SCATTERING WITH AN EFFECTIVE LAGRANGIAN EXPANSION

Similar to the Matzdorf paper, C. E. Aguiar, A. N. F. Aleixo, and C.
A. Bertulani [6], sought to find an equation to describe the motion of
charged particles in the relativistic domain interacting with one another
through the Coulomb field. Unlike Matzdorf, Aguiar et al. attempted to
solve the problem beginning with the Darwin Lagrange, or more accurately,
an expansion of the effective Lagrangian including the Darwin Lagrange.
The derivation of the Darwin Lagrangian was discussed in Section 1.3. We
begin with the full Lagrangian written as:

$$\mathscr{L} = \mathscr{L}^{(0)} + \mathscr{L}^{(2)} \tag{53}$$

where $\mathscr{L}^{(0)}$ is the classical, or zeroth-order Lagrangian and is simply
described as:

$$\mathscr{L}^{(0)} = \frac{\mu v^2}{2} - \frac{Z_1 Z_2 e^2}{r} \tag{54}$$

and $\mathscr{L}^{(2)}$ is the second-order Lagrangian correction, or the Darwin term,
which is written in terms of c^{-2} as:

$$\mathscr{L}^{(2)} = \frac{\mu^4 v^4}{8c^2} \left[\frac{1}{m_1^3} + \frac{1}{m_2^3} \right] - \frac{\mu^2 Z_1 Z_2 e^2}{2m_1 m_2 c^2 r}(v^2 + v_r^2) \tag{55}$$

In both (54) and (55), μ refers to the reduced mass, and in (55),

$v_r = \mathbf{v} \cdot \mathbf{r}/r$. It is clear here that there is a missing third and higher-orders in the Lagrangian. The third-order term describes the dipole radiation emission. Aguiar explains that this term is usually obtained through the Abraham-Lorentz Formalism which is quite mathematically intensive and will not be discussed here. From this formalism, only cases that have equal charge to mass ratios lead to non-runaway solutions, and more specifically, the damping force vanishes entirely. With this assumption, we are able to exclude radiative emissions altogether, and therefore not include a $\mathscr{L}^{(3)}$ term which is the third order term of $\left(\frac{v}{c}\right)$.

By using a standard Hamiltonian, we are able to write a term for the velocity $(d\mathbf{r}/dt)$ and the force $(d\mathbf{p}/dt)$ to the order of c^{-2}, as:

$$\frac{d\mathbf{r}}{dt} = \frac{\mathbf{p}}{\mu} - \frac{p^2}{2c^2}\left[\frac{1}{m_1^3} + \frac{1}{m_2^3}\right]\mathbf{p} + \frac{Z_1 Z_2 e^2}{m_1 m_2 c^2 r}\left[\mathbf{p} + \frac{p_r}{r}\mathbf{r}\right] \tag{56}$$

$$\frac{d\mathbf{p}}{dt} - \frac{Z_1 Z_2 e^2}{r^3}\mathbf{r} + \frac{Z_1 Z_2 e^2}{2m_1 m_2 c^2 r^2}\left[(p^2 + 3p_r^2)\frac{\mathbf{r}}{r} - 2p_r\mathbf{p}\right] \tag{57}$$

where $\mathbf{p}$ is the canonical momentum and can be expressed as:

$$\mathbf{p} = \mu\mathbf{v} + \frac{\mu^4 v^2}{2c^2}\left[\frac{1}{m_1^3} + \frac{1}{m_2^3}\right]\mathbf{v} - \frac{\mu^2 Z_1 Z_2 e^2}{m_1 m_2 c^2 r}\left[\mathbf{v} + \frac{v_r}{r}\mathbf{r}\right] \tag{58}$$

Next, we would like to consider the symmetric system where the charges and the masses of the projectile and target are equal proportions. This simplification allows for a fourth-order correction to the Lagrangian to

be tacked onto (53) which is given by:

$$\mathscr{L}^{(4)} = \frac{mv^6}{512c^4} + \frac{Z^2e^2}{16c^4r}\left[\frac{1}{8}(v^4 - 3v_r^4 + 2v_r^2v^2) + \frac{Z^2e^2}{mr}(3v_r^2 - v^2) + \frac{4Z^4e^4}{m^2r^2}\right]$$

$$\text{where: } \mathscr{L} = \mathscr{L}^{(0)} + \mathscr{L}^{(2)} + \mathscr{L}^{(4)}$$

$$(59)$$

In addition, the equations of motion for the canonical momentum, the velocity, and the force can be derived in the same manner as above, where:

$$\frac{d\mathbf{r}}{dt} = \left[2 - \frac{p^2}{m^2c^2} - \frac{9p^4}{4m^4c^4}\right]\frac{\mathbf{p}}{m}$$
$$+ \frac{Z^2e^2}{m^2c^2r}\left[\left(1 - \frac{p^2}{2m^2c^2}\right)\mathbf{p} + \left(1 + \frac{3p_r^2}{2m^2c^2}\right)\frac{p_r}{r}\mathbf{r}\right] + \frac{Z^4e^4}{m^3c^4r^2}\mathbf{p}$$

$$(60)$$

and,

$$\frac{d\mathbf{p}}{dt} = \frac{Z^2e^2}{r^3}\mathbf{r} + \frac{Z^2e^2}{2m^2c^2r^2}\left[p^2 + 3p_r^2 - \frac{p^4}{4m^2c^2} + \frac{15p_r^4}{4m^2c^2}\right]\frac{\mathbf{r}}{r}$$
$$- \frac{Z^2e^2p_r}{m^2c^2r^2}\left[1 + \frac{3p_r^2}{2m^2c^2}\right]\mathbf{p} + \frac{Z^4e^4p^2}{m^3c^4r^4}\mathbf{r} - \frac{3Z^6e^6}{4m^2c^4r^5}\mathbf{r}$$

$$(61)$$

where the canonical momentum is written as:

$$\mathbf{p} = \frac{1}{2}\left[1 + \frac{v^2}{8c^2} + \frac{3v^4}{128c^4}\right]m\mathbf{v}$$
$$- \frac{Z^2e^2}{4c^2r}\left[\left(1 - \frac{v^2}{8c^2} - \frac{v_r^2}{8c^2} + \frac{Z^2e^2}{2mc^2r}\right)\mathbf{v} + \left(1 - \frac{v^2}{8c^2} + \frac{3v_r^2}{8c^2} - \frac{3Z^2e^2}{2mc^2r}\right)\frac{v_r}{r}\mathbf{r}\right]$$

$$(62)$$

From here, Aguiar performs the numerical analysis of equations of

motion not assuming equal charge to mass ratios, equations (56) and (57). We preform our own analysis of this result in Chapter 6.

We would then like to consider the more simple case of a light particle scattering off a much heavier particle. In this case, because recoil can be neglected (in addition to keeping with the assumption from above: not allowing radiation emission), the retardation effects vanish. This is due to the immobile larger particle, considered to have infinite mass as compared to the other. This causes the field of the heavy particle to also be static. Relativity cannot be entirely ignored however, because of the increase in the mass of the lighter particle due to relativity. We begin our consideration of this case by stating the scattering angle θ is given by:

$$\theta = \pi - \frac{2\eta}{\sqrt{\eta^2 - \beta^2}} \arctan \sqrt{\eta^2 - \beta^2} \tag{63}$$

where η is merely the abbreviation:

$$\eta = \frac{vL}{Z_1 Z_2 e^2} \tag{64}$$

where L, as before, is the angular momentum. As discussed in Chapter 2, in elastic collisions, angular momentum is conserved. Thus the angular momentum must be equal to the linear momentum multiplied by the impact parameter, $L = pb$. From this logic, η is a function of L and therefore a function of b. Because we ultimately would like to solve the differential cross section, which relates b and θ, this leads us to expand η, as

a function of θ, to the second order of β explicitly in addition to a term representing the consolidated higher order terms, $\mathcal{O}(\beta^4)$. This expansion is then plugged into (37) where η, as a function of the impact parameter, replaces b in the following way:

$$\frac{d\sigma}{d\Omega} = \left[\frac{Z_1 Z_2 e^2}{2mv^2 \sin^2(\theta/2)}\right]^2 [1 - h(\theta)\beta^2 + \mathcal{O}(\beta^4)] \tag{65}$$

where $h(\theta) = 1 + \frac{1}{2}[1 + (\pi - \theta)\cot\theta]\tan^2\frac{\theta}{2}$ and in this case, m is the relativistic mass. The last step performed, was to express (65) in terms of the kinetic energy, K.

$$\frac{d\sigma}{d\Omega} = \left[\frac{Z_1 Z_2 e^2}{4K \sin^2(\theta/2)}\right]^2 \cdot \left[1 + g(\theta)\frac{K}{mc^2} + \mathcal{O}\left(\frac{K^2}{(mc^2)^2}\right)\right] \tag{66}$$

where $g(\theta) = 3 - 2h(\theta)$. It is evident that the first term in the brackets is the classical Rutherford scattering formula. The term that follows is Aguiar's proposed relativistic correction to the differential cross section. This final method proposed by Aguiar, although bulky, can be solved analytically without the need for numeric computational methods.

Should the analytic solutions presented in either method above prove to be sufficiently close to the according numeric solution, then the time costly numeric solution would not be necessary. This is discussed for both methods in Chapter 6, Results. Before we discuss the results of our investigation, we need to review the numerical method we employed to solve the numeric solutions presented.

Chapter 5

RUNGE KUTTA NUMERICAL METHOD

5.1   Basic Runge Kutta Method

The last bit of background necessary to discuss is an extremely useful numerical method, called the Runge Kutta method. This method is used to solve ordinary first order differential equations of the form:

$$\frac{dy}{dx} = f(x, y) \tag{67}$$

If we attempt to solve this differential equation over some small interval of $i \to i+1$ (what is considered small depends entirely on the function) we would proceed by:

$$
\begin{aligned}
dy =& f(x, y)dx \\
\int_{y_i}^{y_{i+1}} dy =& \int_{xi}^{x_{i+1}} f(x, y)dx \\
y_{i+1} - y_1 =& \int_{xi}^{x_{i+1}} f(x, y)dx \\
y_{i+1} =& y_i + \int_{x_i}^{x_{i+1}} f(x, y)dx
\end{aligned}
\tag{68}
$$

under the assumption of a non-precipitous function, or at least relatively smooth over the required interval, the integral in the last term can be reduced to the slope of the function, ϕ multiplied by the horizontal

displacement or the step interval, h, reducing the equation to:

$$y_{i+1} = y_i + \phi h \tag{69}$$

This is the form of the simplest Runge Kutta scheme, and is of the first order. The second order is solved using something that is very similar to (69), but the slope is modified to be $\phi = (a_1 k_1 + a_2 k_2)$ where a_1 and a_2 are constants, and $k_1 = f(x_i, y_i)$ and $k_2 = f(x_i + p_1 h, y_i + q_{11} k_1 h)$ where p_1 and q_{11} are also just constants. We would like to find out what all of these constants are, and to do this we use a Taylor expansion of (69) about the point y_i including the new ϕ, where $y_{i+1} = y_i + f(x_i, y_i)h + \frac{f'(x_i,y_i)}{2!}h^2 + \dots$ and what this does, is it allows us to apply some constraints to the mess of constants we have in the following way:

$$
\begin{aligned}
a_1 + a_2 &= 1 \\
a_2 \cdot p_1 &= \frac{1}{2} \\
a_2 \cdot q_{11} &= \frac{1}{2}
\end{aligned}
\tag{70}
$$

From here, we employ a classic solution to solve the remaining portions of (70) called the Midpoint method where we artificially set $a_2 = \frac{1}{2}$. This then solves the remainder of the constants where $a_1 = \frac{1}{2}$, $p_1 = 1$, and $q_{11} = 1$. There are three broadly adopted methods, Heun's Method where you set $a_2 = \frac{1}{2}$, the Midpoint Method mentioned above, and the Ralston's Method where you set $a_2 = \frac{2}{3}$. These are all valid methods,

but the Midpoint method specifically involves using the derivative at the starting point, and using that to approximate the derivative at the midpoint. This slope at the midpoint is then used in a straight line approximation from the original location to find the new position location after a step h. As an example, the midpoint method we will use from here on. It then follows that (69) becomes:

$$y_{i+1} = y_i + k_2 \tag{71}$$

where $k_1 = hf(x_i, y_i)$ and $k_2 = hf(x_i + \frac{1}{2}h, y_i + \frac{1}{2}k_1)$

5.2   Adaptive Step Size Runge Kutta Method

We would now like to consider an adaptive solution that tries to take into account the inherent error associated with approximating the solutions of differential equations. In these methods, it seems obvious that as the step size decreases, accuracy increases. The natural response is then to have $h \to 0$. This has a problem however, in that as h gets smaller, the computation time increases, so it is not realistic to have $h = 0$, because that would then require infinite computation time. In most cases however, we do not need the exact answer; we merely need an answer that is sufficiently close to the exact answer, within some acceptable margin of error. Additionally, error can be reduced by using higher order methods. The last problem we seek to address is that of uneven error that occurs as a curve

transitions from relatively smooth to steep (or vise versa). If the local error, or the instantaneous error associated with each point, was uniform, that would greatly improve any approximation. To achieve this, we introduce what is known as an adaptive step size Runge Kutta method.

One of the major tenets of this method is error reduction, so we require a way to estimate the error at each step. The way this is done, is by using two different methods at the same time. The solution that better matches the exact, or known value is assumed to be very close to the exact value, so the method that produced the less accurate values has a local error equal to the absolute difference between the two values. For an example, using different methods, say:

$$\text{Method 1: } y_1(x + h)$$
$$\text{Method 2: } y_2(x + h) \tag{72}$$
$$\text{Local Error: } |y_1(x + h) - y_2(x + h)|$$

At this point, if the local error is far below some preset tolerance (usually set by the computation power available to you), then the approximation for this point is more accurate than necessary, meaning it is wasting valuable computation time, and we can double the step size. If the error is far above that tolerance, then we can half the step size to improve the accuracy in this region. Lastly, if the error approximates the tolerance, then the step size is acceptable for this point, and we move on to the next

step.

An example of different methods would simply be to use two methods of different orders, where the higher order method can be assumed to be the more accurate method, and the lower order method to be assumed to be less accurate. Two such methods could be Runge Kutta second order approximation (71) and the Runge Kutta third order approximation (not discussed here). In this example, the third order Runge Kutta is considered to be essentially exact, and the error is calculated by finding the difference between the value of the third order approximation and the second order.

Chapter 6

RESULTS

6.1 Numerical Results

We seek to investigate Matzdorf's [5] solutions to the motion of relativistic, heavy, charged particles interacting, equations (47) and (43), and compare those to Aguiar's [6] solutions, equation (59). We solved these equations numerically using the adaptive step size control Runge Kutta method discussed in Section 5.2. We began by using the same initial conditions as [5], where the target particle is taken to be motionless at the origin at time, $t = -\infty$. The impact parameter, $y(t = -\infty) = b$ where the projectile moves towards the target in the $\hat{x}$ direction; the total trajectory distance is confined to $80,000\ fm$ for our calculations. At time $t = +\infty$ the projectile scatters to an angle θ, with a velocity v_∞ (which is equal to $v_{-\infty}$ from conservation of momentum). These parameters are all nearly identical to the classical scattering parameters discussed in Chapter 2 for reference.

The impact parameter is varied in increments of $\Delta b = 0.1\ fm$ from $60\ fm$ to the sum of the atomic radii of the target and projectile, $R_t + R_p$.

To begin with, the scattering angles obtained using Methods [5] and [6] are checked against well known classical, non-relativistic Rutherford scattering angle $\theta^{(c)}$, [8]:

$$\theta^{(c)} = 2\arctan\left(\frac{q_p q_t}{\mu v^2 b}\right) \tag{73}$$

In Figure 4 and Figure 5, a ^{208}Pb $+^{208}$ Pb collision is shown with the relative percent difference between each method, with the classical deflection angle presented as a percent difference:

$$\% = \left| \frac{\theta^{[5]or[6]} - \theta^{(c)}}{\theta^{(c)}} \right| \times 100 \tag{74}$$

plotted against the impact parameter in Figure 4 at 100 MeV per nucleon, and in Figure 5, plotted against the bombarding energy, E_{lab} in MeV per nucleon at a grazing impact parameter equal to the sum of the atomic radii of the target and projectile.
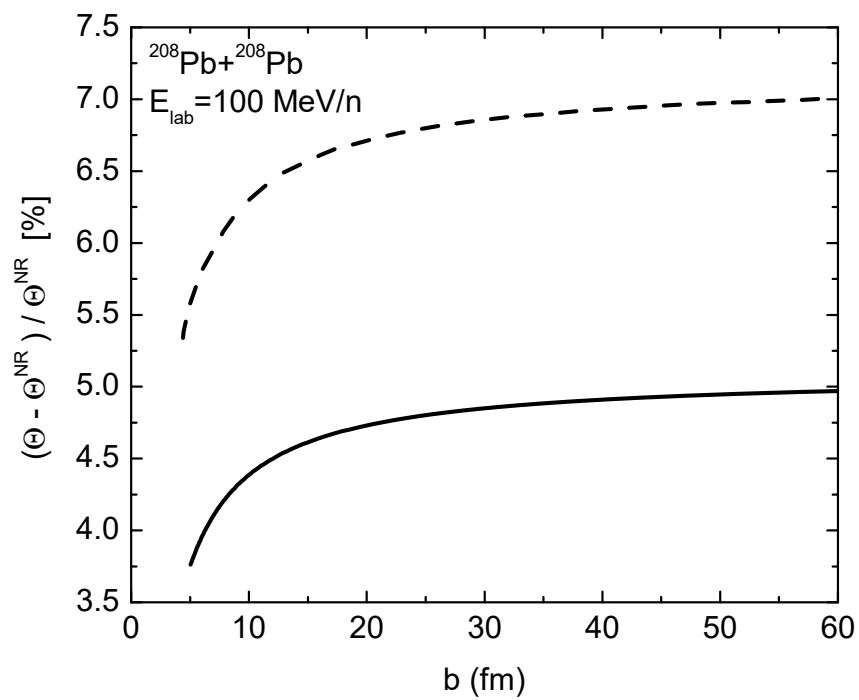
Figure 4: ^{208}Pb $+^{208}$ Pb collision at $100\frac{MeV}{n}$. Scattering angle percent difference vs. impact parameter.
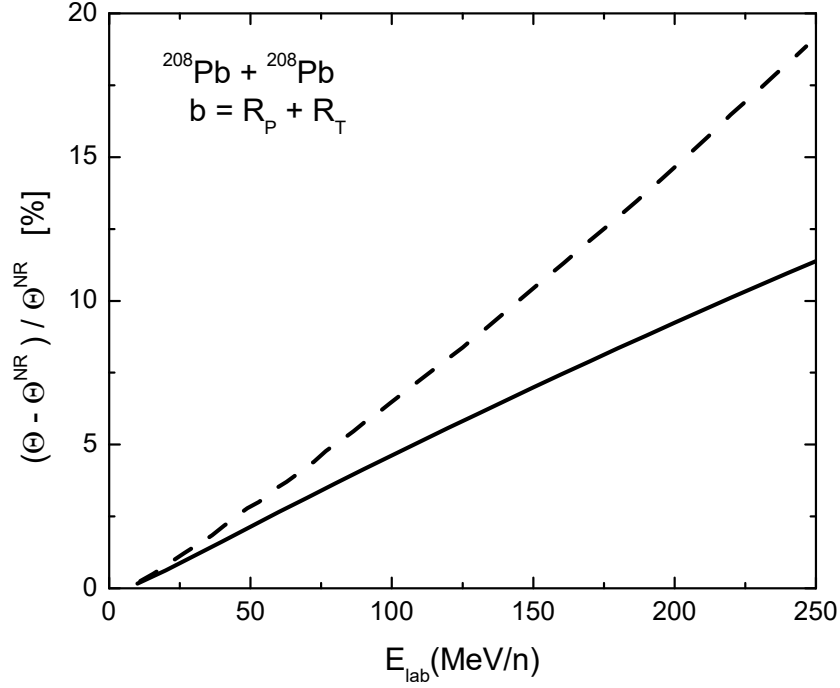
Figure 5: ^{208}Pb $+^{208}$ Pb collision at $b = R_p + R_t$. Scattering angle percent difference vs. bombarding energy.

The dashed line represents the Aguiar method to order $\left(\frac{v}{c}\right)^4$, allowed to this order because of the equal charge to mass ratio as shown in [5], and the solid line represents the Matzdorf method. From Figure 4, it is evident that the Matzdorf method compares more closely to the non-relativistic scattering angle than the method of Lagrangian expansion by Aguiar. Because of the known, small contribution from the magnetic field, the smaller deviation from the non-relativistic angle in Matzdorf's method can be attributed to their non-inclusion of the magnetic terms, while the

Darwin Lagrangian relies heavily on the magnetic field. Figure 4 also shows that the scattering angle % difference increases as b increases, but the percent caps at about $\sim 7\%$ for Aguiar's method; and caps at about $\sim 5\%$ for Matzdorf's method. This cap in the percentage is an intuitive result because at larger impact parameters, the defection angle decreases for both methods as well as the Rutherford classical scattering at approximately the same rate after small impact parameters. Therefore the percent difference should cap asymptotically as $b \to \infty$.

In Figure 5 it is clear that both methods increasingly deviate from the Rutherford classical scattering angle as the bombarding energy increases. This is perfectly reasonable to expect, as retardation and relativistic corrections cause substantial deviations from the classical solutions as we approach the relativistic domain. Once again, this figure shows that the Aguiar method exceeds the percent difference in the scattering angle as compared to that of the Matzdorf method. This is most likely due to Aguiar's consideration of relativistic mass but reduced consideration of retardation associated with this method.

Next, a comparison is made to the classical differential cross section, $\left(\frac{d\sigma}{d\Omega}\right)^{(c)}$ displayed in the same method as above in the form of a percent difference between the two methods and the classical cross section. These are displayed in Figure 6 and Figure 7 where the former shows a $^{208}\text{Pb} + ^{208}\text{Pb}$ collision at 100 MeV per nucleon plotted against the scattering angle, while the latter shows the same Lead collisions plotted

against the laboratory energy at a grazing impact parameter.
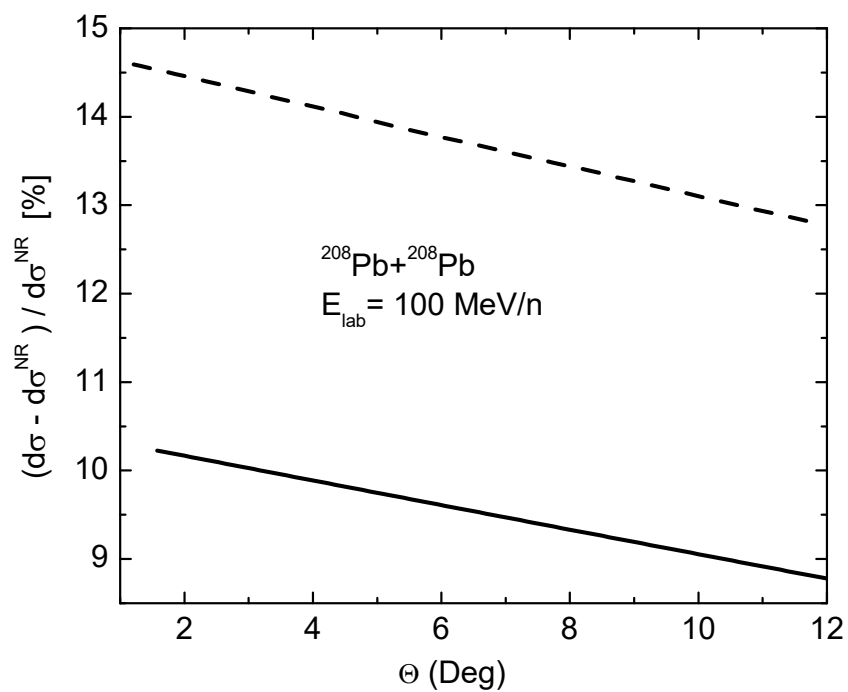
Figure 6: ^{208}Pb +^{208} Pb collision at $100\frac{MeV}{n}$. Differential scattering cross section percent difference vs. scattering angle.
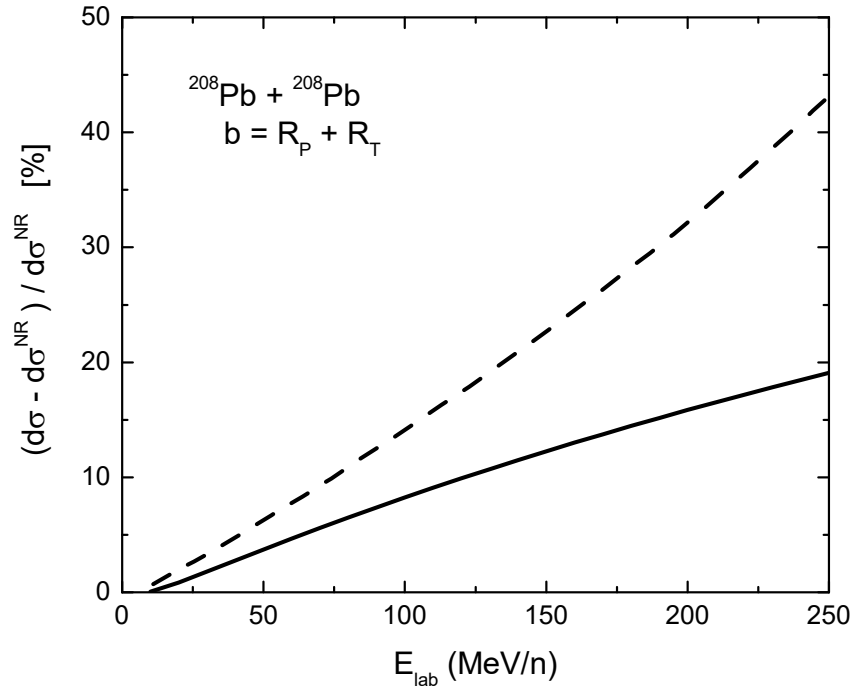
Figure 7: ^{208}Pb $+^{208}$Pb collision at $b = R_p + R_t$. Differential scattering cross section percent difference vs. bombarding energy.

It is clear from Figure 6 that the two methods' solutions for the differential scattering cross section are quite far apart from one another when they are plotted against the scattering angle ($\sim 4.5\%$). Once again, the dashed line represents Aguiar's method, and the solid line represents Matzdorf's method. It should be noted that each method becomes more like the classical scattering as the scattering angle is increased. This is can be accounted for by a close look at the classical differential scattering cross section. The differential scattering cross section, being proportional to the

probability that the particle is scattered to a differential solid angle from a differential cross sectional area, should decrease very rapidly as the scattering angle increases. More succinctly, you would expect fewer deflections to high angles, and more deflections at low angles. However, at higher energies, you would expect smaller deflection angles for the aggregate, regardless of the impact parameter, but it would still drop off rapidly. We would therefore expect the higher classical differential scattering cross sections for higher scattering angles than that of the relativist methods, but both should approach zero as the deflection angle increases. This should manifest itself as a negative slope on the percent difference vs. angle plot. As is evident by the data from Figure 6, the curve does indeed drop off as the scattering angle increases, which is exactly what we should expect.

Similar to Figure 5, Figure 7 shows that both methods increasingly depart from the classical differential cross section as the laboratory energy is raised. As before, Matzdorf's method does not deviate from the classical differential as much as Aguiar's method for both Figure 6 and 7.

For all the numeric solutions presented for symmetric collisions, both methods are in close proximity to one another, and agree well with the classical regime at low energies. Matzdorf's solution is far more close to the classical Rutherford solution in all of the figures presented.

6.2   Analytic Results

As both methods are presented with two possible solutions: a more involved solution that requires a numerical method approach (the previous section), and a less involved analytic solution, it seems prudent to also compare these more time efficient methods to see if they hold muster. First we examine the differential scattering cross section produced by each method for the same symmetric collision of ^{208}Pb $+^{208}$ Pb at a grazing angle $b = R_p + R_t$. This is a pure solution graphic, not a comparison to the classical differential scattering cross section in the form of a percent as before.
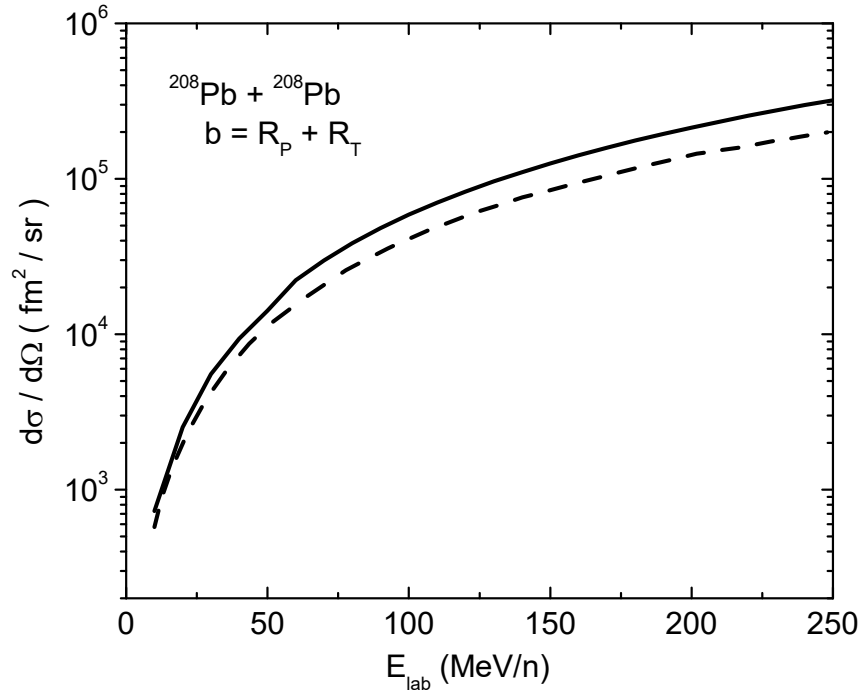
Figure 8: $^{208}\text{Pb} + {}^{208}\text{Pb}$ collision at $b = R_p + R_t$. Differential scattering cross section vs. bombarding energy.

Figure 8 shows that both methods agree very closely at low energies and separate only slightly at higher energies. It should be noted that the vertical axis, which displays the differential scattering cross section, is logarithmic. This can make large differences seem smaller, but the two methods are in relatively good agreement.

The analytic formulas proposed by both papers are valid for light particles scattering off a heavy target. In Figure 9 the differential scattering cross section percent difference is plotted against the scattering angle for

the asymmetric collision of ^{17}O $+^{208}$ Pb. Due to the asymmetry, Aguiar's method is only valid up to order of $\left(\frac{v}{c}\right)^2$.
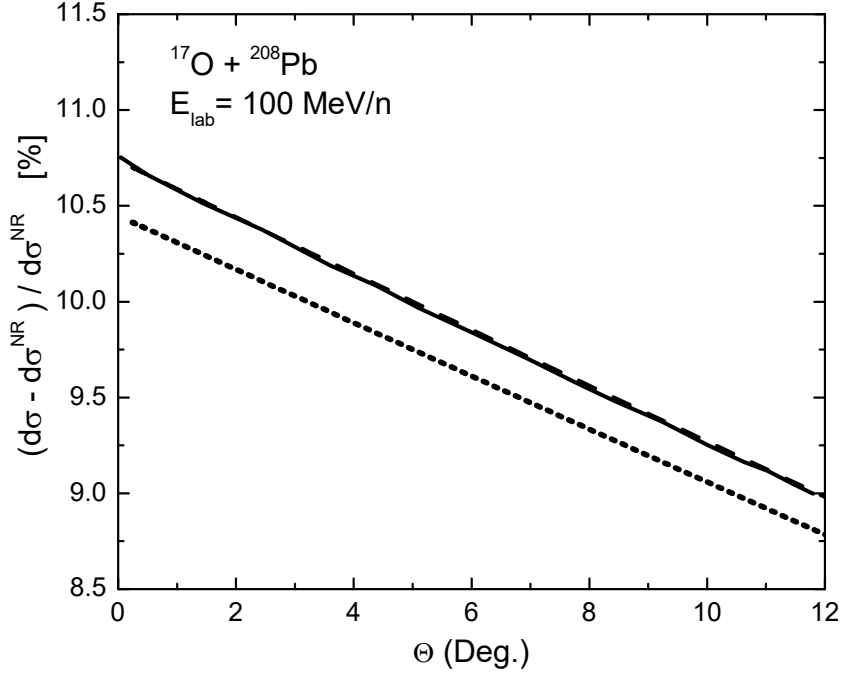
Figure 9: ^{17}O$+^{208}$Pb collision at $100\frac{MeV}{n}$. Differential scattering cross section percent difference vs. scattering angle.

Figure 9 shows three different lines. The dashed line represents Aguiar's analytic solution (65), while the solid line represents Aguiar's exact, numeric solution up to the order of $\left(\frac{v}{c}\right)^2$. These are both in excellent agreement with one another. The dotted line represents Matzdorf's analytic equations (51). Not shown in this graphic is the Matzdorf numeric exact result, which would lie on-top of the dotted line, and would be

indistinguishable from Matzdorf's solutions at this resolution; it agrees within 0.1% of that of the exact result.

It is clear from Figure 9 that the two methods are in much better agreement with one another for light on heavy particle collisions. Not only do the analytic methods presented by Aguiar and Matzdorf agree well with one another, they also agree quite well with the exact result of the numeric solutions, the consequences of which are discussed in Chapter 7.

6.3 Analysis of the Distance of Closest Approach

We first start by defining half the distance of closest approach in a head on non-relativistic collision, a_0 , which is a useful scattering parameter characterized by:

$$a_0 = \frac{q_p q_t}{\mu v^2} \tag{75}$$

To begin a study of the distance of closest approach, it is convenient to first employ the use of a helpful parameterization common to orbital motion problems:

$$
\begin{aligned}
x &= a_0(\cosh \omega + \epsilon) \\
y &= a_0 \sqrt{\epsilon^2 - 1} \sinh \omega \\
z &= 0
\end{aligned}
\tag{76}
$$

where ω is the angular frequency and ϵ is the eccentricity which is related to the scattering angle by $\epsilon = \sin^{-1}(\frac{\theta}{2})$. Then if we wish to express this

parameterization in terms of the radial distance $r = \sqrt{x^2 + y^2 + z^2}$, then we arrive at $r = a_0(\epsilon \cosh \omega + 1)$. Then by solving $v = \frac{dr}{dt} = \frac{dr}{d\omega} \cdot \frac{d\omega}{dt}$ and rearranging for t, we attain the useful time parameterization:

$$t = \frac{a_0}{v}(\epsilon \sinh \omega + \omega) \tag{77}$$

Next we move this parameterization into the relativistic domain by replacing all instances of a_0 with a where $a = \frac{a_0}{\gamma}$. We can finally introduce the relativistic distance of closest approach b_c associated with the impact parameter by:

$$b_c = a + \sqrt{a^2 + b^2} \tag{78}$$

With this, we calculate the impact parameter by solving Matzdorf's equations (51) and the definition of $k(b)$ for the distance of closest approach, labeled b^{Analyt} and compare that to the relativistic distance of closest approach in a similar manner as the prior figures, in the form of a percent difference. These are displayed in Figure 10.
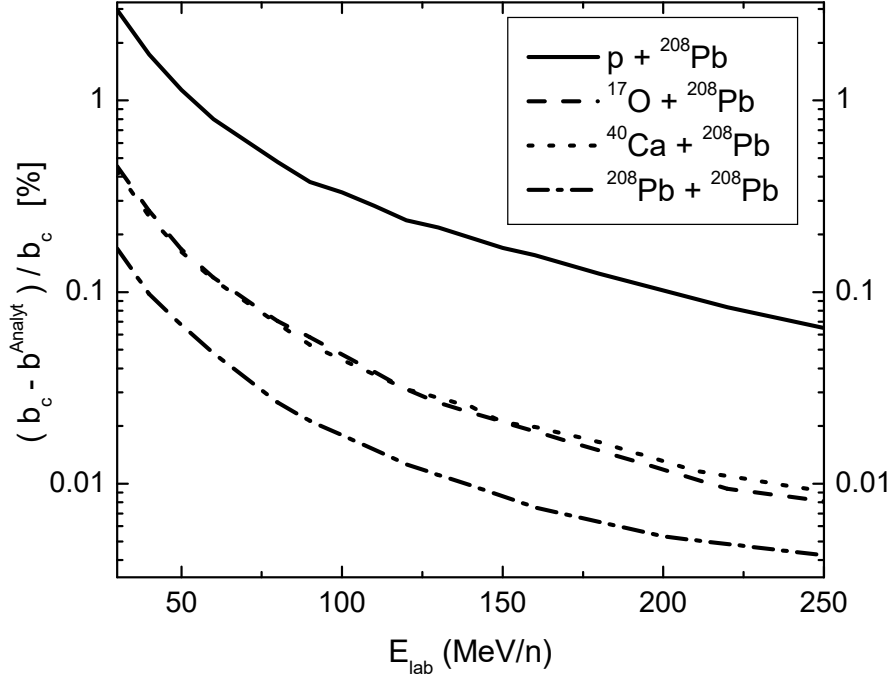
Figure 10: Multiple different collisions at $b = R_p + R_t$. Distance of closest approach percent difference vs. bombarding energy.

The solid line represents a p $+^{208}$Pb collision (p is a single proton), the dashed line represents a ^{17}O $+^{208}$Pb collision, the dotted line represents a ^{40}Ca $+^{208}$Pb collision, and the dashed-dotted line represents the symmetric ^{208}Pb $+^{208}$Pb collision; all of which were evaluated at a grazing impact parameter. The accuracy of these collisions is excellent even for the severely asymmetric case. Equation (78) therefore, produces a result very close to the "exact" result, all at or below the accuracy of 1% or less, further showing the validity of Matzdorf's methods.

Chapter 7

CONCLUSIONS

In this paper, we have reviewed methods for solving for the relativistic motion of heavy-on-heavy and light-on-heavy ion collisions. These collisions were evaluated over a spread of impact parameters, bombardment energies, and scattering angles; and from these the differential scattering cross section and the relativistic distance of closest approach were calculated and plotted.

Through a thorough investigation of the relativistic effects manifested in the form of the magnetic interactions included in the Coulomb scattering, the retardation of the Coulomb electric potential, and the change in mass due to relativistic speeds, we have reached a a few important interpretations from our results. The solutions to the scattering angle and differential scattering cross section presented by Matzdorf [5] as a solution to the covariant equations of motion are shown to be markedly better than the method of Lagrangian expansion by orders of $\frac{v}{c}$ outlined by Aguiar et al. [6]. The covariant equation solution accounts for retardation very well, while the Lagrangian expansion does not. The effects of retardation being quite large in relativistic motion, this is something that needs to be considered in high energy elastic scattering. In addition to this, the inclusion of magnetic interaction terms proves to be unnecessary, as its contributions are negligible to the motion of relativistic ions. This could be

further reason for the superiority of the Matzdorf method, as the Lagrangian expansion includes the Darwin Lagrangian, which is heavily influenced by magnetic terms.

Further, the Matzdorf's analytic solutions were found to be in good enough agreement with the corresponding numeric solutions of equations (43) and (47). The differential scattering cross section has been shown to be best described using equation (52). The scattering angle is solved most efficiently using equation (51). Lastly, the relativistic distance of closest approach, which is described in equation (78), in addition to the time dependence parameterization of the trajectory, given by equations (76), are shown to agree very well with one another.

In summation, the solution of the covariant equation of a charged particle moving in the external electromagnetic field of another charged particle method for accounting for the elastic scattering of heavy ions is more effective than the method of Lagrangian expansion. In addition, the analytic formulation following the covariant equation solution method is sufficient for all circumstances tested. Therefore, the more computationally involved numerical method is not necessary even for the severely asymmetric cases.

REFERENCES

[1] Darwin C. G., *Philos. Mag Ser. 6*, 39, p. 537, 1920.

[2] Jackson J. D., 1999, *Classical Electrodynamics*, 3rd edition (John Wiley & Sons, New York).

[3] Essén H., 2005, *Eur. J. Phys.*, 26, p. 279.

[4] Rutherford E., May 1911, *The Scattering of α and β Particles by Matter and the Structure of the Atom*, Philosophical Magazine. Series 6, 21.

[5] Matzdorf R., Soff G.,Mehler G., 1987, *Elastic Collisions of Heavy Ions at Intermediate Energies*, Zeitschrift Physik D Atoms, Molecules and Clusters, 6, Number 1, pp. 5-12.

[6] Aguiar C. E., Aleixo A. N. F., Bertulani C. A., November 1990, *Elastic Coulomb Scattering of Heavy Ions at Intermediate Energies*, American Physical Society Physics Review C, 42, iss. 5.

[7] Sommerfeld A., 1978, *Atombau und Spektrallinien*. Frankfurt: Harri Deutsch.

[8] Goldstein H., Poole C., Safko J., 2002, *Classical Mechanics*, 3rd edition (Addison Wesley), p. 110

VITA

George Phillip Robinson attended Angelo State University in San Angelo, Texas where he received his Bachelors of Science in Physics in May of 2015. George further continued his education obtaining a Masters of Science in Physics from Texas A&M University-Commerce in Commerce, Texas in August of 2017.